Journal of Computer Methods in Civil Engineering
Volume 1 Issue 1 No. 2
Received 12 April 2022; Accepted 13 June 2022
Published Online June 28 2022

# Numerical analysis on characteristics of acoustic emission signals in bridge cables based on semi-analytic FEM

**Yaohua Yang[1, *], Limin Sun[2]**
[1]Department of Bridge Engineering, Tongji University, Shanghai, China
[2]State Key Laboratory for Disaster Reduction in Civil Engineering, Tongji University, Shanghai, China

**Abstract.** Acoustic emission (AE) signal, actually, is the phenomenon of stress wave propagation in steel wires in bridge cables. The Semi-Analytical Finite Element (SAFE) method serves as a powerful tool for analyzing wave characteristics in most, if not all, of waveguides. In this paper, the SAFE method for circular cross-section waveguide was established in section 2. The frequency-spectrums, energy velocity and attenuation coefficient curves for viscoelastic steel wires can be obtained readily. Based on the method, the effects of initial tensile stress were studied in section 4. It demonstrates that tensile stress tends to increase energy velocities and decrease attenuations in regions above cut-off frequencies.

**Keywords.** Acoustic emission (AE), Semi-Analytical Finite Element (SAFE) method, wave modes, cables

## 1 Introduction

The theoretical frequency equation for wave motion in an infinite circular cylinder, proposed by J.Pochhammer in1876 and C.Chree in1889[1] generally serves as the foundation of single steel wire research. However, due to the difficulties and numerical instabilities in solving the equation, its applicability is constrained. The SAFE method is an effective substitution for the theoretical method. In SAFE method, the cross section of a waveguide is supposed to be discretized by normal Finite Element Method (FEM) procedure, while the wave functions related to space and time domain are retained. Numerous researchers have contributed brilliant work on developing the method. Nelson, Dong[2] firstly formulated SAFE method for layered orthotropic cylinders and plates with a mono-dimensional element. Gavrić, L[3] , Hayashi, T[4] expanded the method to steel rails with a bi-dimensional element. Bartoli, I[5] , furthermore, considered arbitrary cross sections of viscoelastic materials and Marzani, A[6] applied the axisymmetric SAFE method on multi-layered anisotropic axisymmetric waveguides.

In the present work, the axisymmetric SAFE method has been introduced to analyze the wave characteristics of a high tensile strength steel wire with 5mm diameter, typically used in actual cables, in section 2. In section 3, the full frequency spectrums, energy velocity and attenuation curves of the steel wire are obtained. Finally, the influences of initial tensile stress on viscoelastic steel wire are studied based on the method.

## 2 The SAFE method

### 2.1 Mathematical framework

The wave modes in an infinite cylinder can be classified into three types, namely flexural mode, longitudinal mode and torsional mode, noted as $F(n,m)$, $L(0,m)$, $T(0,m)$ respectively, in which $n$ and $m$ stand for circumferential number and frequency order number. In cylindrical coordinate, the theoretical displacement fields of three types of wave modes can be written as below respectively

$$\begin{cases} u_r = U(r)\cos(n\theta)\exp\big(i(kz-\omega t)\big) \\ u_\theta = V(r)\sin(n\theta)\exp\big(i(kz-\omega t)\big) \\ u_z = W(r)\cos(n\theta)\exp\big(i(kz-\omega t)\big) \end{cases} \quad \begin{cases} u_r = U(r)\exp\big(i(kz-\omega t)\big) \\ u_z = W(r)\exp\big(i(kz-\omega t)\big) \end{cases} \quad u_\theta = V(r)\exp\big(i(kz-\omega t)\big) \tag{1}$$

where $r,\theta,z$ stand for radius, circumferential, and axial coordinates respectively, $k,\omega,t$ stand for wavenumber, circular frequency and time respectively, finally $i$ denotes the virtual unit. Substituting $\boldsymbol{u}=[u_r,u_\theta,u_z]^T$, in which superscript $T$ denotes transpose, into the classical geometric equation $\boldsymbol{\varepsilon}=\boldsymbol{L}\boldsymbol{u}$ and constitutive equation $\boldsymbol{\sigma}=\boldsymbol{D}\boldsymbol{\varepsilon}$, the strain field $\boldsymbol{\varepsilon}=[\varepsilon_r \quad \varepsilon_\theta \quad \varepsilon_z \quad \gamma_{r\theta} \quad \gamma_{\theta z} \quad \gamma_{zr}]^T$ and stress field $\boldsymbol{\sigma}=[\sigma_r \quad \sigma_\theta \quad \sigma_z \quad \tau_{r\theta} \quad \tau_{\theta z} \quad \tau_{zr}]^T$ of a certain wave mode can be obtained as well. $\boldsymbol{L}$ and $\boldsymbol{D}$ are compatibility operator in cylindrical coordinate and constitutive matrix which will be complex in terms of viscoelastic materials. For the SAFE method, however, applying the virtual work principle with the equations above, also discretizing the displacement fields in radius direction with matrix $\boldsymbol{N}$ of mono-dimensional quadratic interpolation function, leads to

*Corresponding author. Tel.: +86-21-65980952; E-mail address: lmsun@tongji.edu.cn
National Natural Science Foundation of China (No.51478347)

$$\left\{\sum_{i=1}^{N_{el}}\int_{-\infty}^{+\infty}\int_{0}^{2\pi}\int_{R_i}^{R_{i+1}}\left[\delta\left(\boldsymbol{LNu}\right)^{T*}\boldsymbol{D}\left(\boldsymbol{LNu}\right)-\omega^2\delta\left(\boldsymbol{LNu}\right)^{T*}\rho\left(\boldsymbol{LNu}\right)\right]rdrd\theta dz\right\}=0 \quad (2)$$

where the asterisk denotes conjugate, $N_{el}$ is the total number of elements, and $l_i = R_{i+1} - R_i$ is the length of $i$ th element. After some algebraic calculations, including applying the orthogonality of trigonometric functions and the normal element assembling procedures, the frequency equation can be expressed as a quadratic eigenvalue system below

$$\left[\boldsymbol{K}_1\left(n,\theta\right)+ik\left(\boldsymbol{K}_2\left(n,\theta\right)-\boldsymbol{K}_2^T\left(n,\theta\right)\right)+k^2\boldsymbol{K}_3\left(n,\theta\right)-\omega^2\boldsymbol{M}\left(n,\theta\right)\right]\boldsymbol{U}=0 \quad (3)$$

The system can also be converted into a first-order one by doubling its size

$$\left[\boldsymbol{A}\left(n,\omega\right)-k\boldsymbol{B}\left(n,\omega\right)\right]\boldsymbol{Q}=0 \quad (4)$$

where

$$\boldsymbol{A}\left(n,\omega\right)=\begin{bmatrix}\boldsymbol{0} & \boldsymbol{K}_1-\omega^2\boldsymbol{M}\\ \boldsymbol{K}_1-\omega^2\boldsymbol{M} & i\left(\boldsymbol{K}_2-\boldsymbol{K}_2^T\right)\end{bmatrix}\quad \boldsymbol{B}\left(n,\omega\right)=\begin{bmatrix}\boldsymbol{K}_1-\omega^2\boldsymbol{M} & \boldsymbol{0}\\ \boldsymbol{0} & -\boldsymbol{K}_3\end{bmatrix}\quad \boldsymbol{Q}=\begin{bmatrix}\boldsymbol{U}\\ k\boldsymbol{U}\end{bmatrix} \quad (5)$$

Specially, with respect to longitudinal mode and torsional mode, the derivation is much simpler than the procedures of flexural modes, since they only possess two degrees of freedom (DOFs) and one DOF respectively in each single node. Also the trigonometric functions disappear in the displacement expressions.

## 3 Solutions to viscoelastic steel wires

Regarding viscoelastic materials, all wavenumbers are complex, which means each mode possesses attenuation coefficients. In this case, only equation(4) can be applied to solve the eigensystem as $k = k(\omega)$ . The real part of a wavenumbers represents wave oscillation in space domain while its imaginary part, also known as attenuation coefficient $att$ , describes amplitude decaying. Generally, most of AE signals received by sensors are those of propagative modes with low attenuation.

In terms of the viscoelastic materials, the damping properties are introduce by complex Young's modulus and Poisson's ratio

$$\tilde{E}=\rho\tilde{c}_s^2\left(\frac{3\tilde{c}_l^2-4\tilde{c}_s^2}{\tilde{c}_l^2-\tilde{c}_s^2}\right)\quad \tilde{\nu}=\frac{1}{2}\left(\frac{\tilde{c}_l^2-2\tilde{c}_s^2}{\tilde{c}_l^2-\tilde{c}_s^2}\right) \quad (6)$$

where $\tilde{c}_l$ and $\tilde{c}_s$ are complex bulk longitudinal and shear wave velocity, defined as

$$\tilde{c}_{l,s}=c_{l,s}\left(1+i\frac{\kappa_{l,s}}{2\pi}\right)^{-1}\quad c_s=\sqrt{\mu/\rho}\quad c_l=\sqrt{\left(2\mu+\lambda\right)/\rho} \quad (7)$$

$\mu$ and $\lambda$ are Lame constants, $\kappa_l$ and $\kappa_s$ are bulk longitudinal and shear wave attenuation coefficients, for high tensile strength steel wire that $\kappa_l = 0.003Np/\lambda$ , $\kappa_s = 0.008Np/\lambda$ . The figures below present the full frequency spectrum curves of $L_d(0,m)$ and $F_d(1,m)$ of a viscoelastic steel wire with 5mm diameter, in which subscript $d$ represents damp

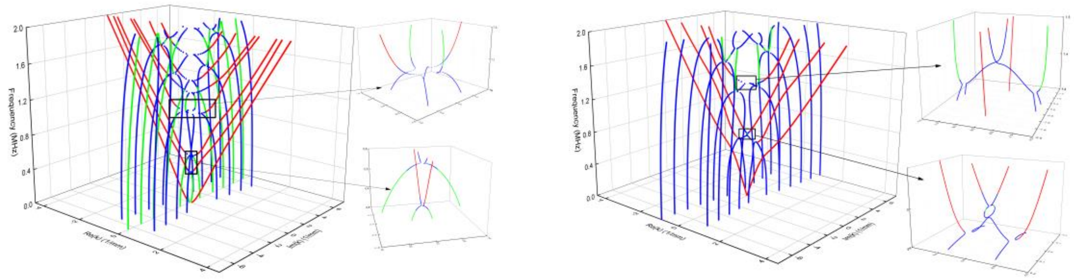

(a) (b)

**Figure 1.** Full frequency spectrum curves of a viscoelastic steel wire

(a) $F_d(1,m)$ mode; (b) $L_d(0,m)$ mode

(Red line: $|k_{\mathrm{Re}}/k_{\mathrm{Im}}| > 100$ ; blue line: $0.01 \le |k_{\mathrm{Re}}/k_{\mathrm{Im}}| \le 100$ ; green line: $|k_{\mathrm{Re}}/k_{\mathrm{Im}}| < 0.01$ )

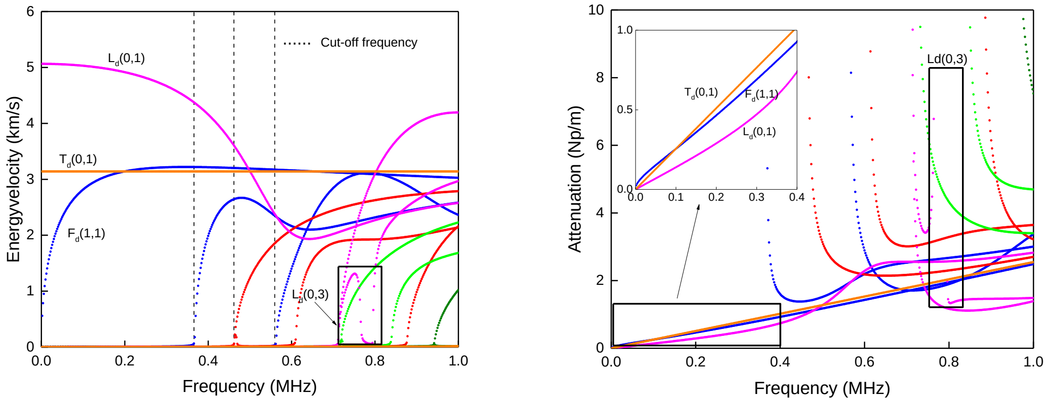


(a) Energy velocity curves (b) Attenuation coefficients curves (low area)

**Figure 2.** Dispersion curves of 5mm-diameter steel wire with damp

It can be seen in Figure 1 that the curves separate with each other automatically, being consecutive along with frequency axis. Additionally, because of the automatic separations, mode tracking can be readily and clearly achieved. In this case, every single curve possesses same signs of $att$ which means the modes affiliated to a same curve all travel in a same direction. Energy velocity is able to describe transmission of energy in waveguides, defined as

$$C_e = \int_{\Omega} P_z / (S + K)\, d\Omega \tag{8}$$

in which

$$\int_{\Omega} P_z d\Omega = \omega \operatorname{Re}\left(-i\boldsymbol{U}^{T*}\boldsymbol{K}_2^T\boldsymbol{U} + k\boldsymbol{U}^{T*}\boldsymbol{K}_3\boldsymbol{U}\right)/2 \quad \boldsymbol{P} = \left[P_r \quad P_\theta \quad P_z\right]^T = -\operatorname{Re}\left(\bar{\boldsymbol{\sigma}}^*\dot{u}\right)/2 \tag{9}$$

$$\int_{\Omega} S d\Omega = \int_{\Omega}\left[\operatorname{Re}\left((\boldsymbol{\sigma})^{T*}\boldsymbol{\varepsilon}\right)/4\right] d\Omega = \operatorname{Re}\left(\boldsymbol{U}^{T*}\boldsymbol{K}_1\boldsymbol{U} + ik\boldsymbol{U}^{T*}\boldsymbol{K}_2\boldsymbol{U} - ik^*\boldsymbol{U}^{T*}\boldsymbol{K}_2^T\boldsymbol{U} + kk^*\boldsymbol{U}^{T*}\boldsymbol{K}_3\boldsymbol{U}\right)/4 \tag{10}$$

$$\int_{\Omega} K d\Omega = \int_{\Omega}\left[\operatorname{Re}\left(\rho(\dot{\boldsymbol{u}})^{T*}\dot{\boldsymbol{u}}\right)/4\right] d\Omega = \omega^2 \operatorname{Re}\left(\boldsymbol{U}^{T*}\boldsymbol{M}\boldsymbol{U}\right)/4 \tag{11}$$

$P_z$ denotes the Poynting vector $\boldsymbol{P}$ of $z$ direction, $\bar{\boldsymbol{\sigma}}$ denotes the classical $3 \times 3$ stress tensor, dot denotes the derivation with respect to time, and $\Omega$ denotes the integration domain of a cross-section. The positive energy velocity and corresponding attenuation curves are shown in Figure 2.

Since the curves are consecutive along frequency axis as mentioned before, the energy velocity curves are extended to original point. It can be seen that the energy velocities below the cut-off frequencies are extremely small, which indicates they cannot carry propagative energies. Except the three curves of elementary modes $F_d(1,1), L_d(0,1), T_d(0,1)$ and $L_d(0,3)$, the attenuation curves of other modes tend to firstly decrease with the increase of frequency up to minimums of which frequencies are slightly larger than cut-off frequencies, and then increase along frequency axis. The energy and attenuation coefficient curves of flexural modes with same $m$ are assembled as well in Figure 3. The curves with same $m$ possess same trends while attenuations of modes with higher circumferential numbers are larger in high frequency area in each group.

(a)

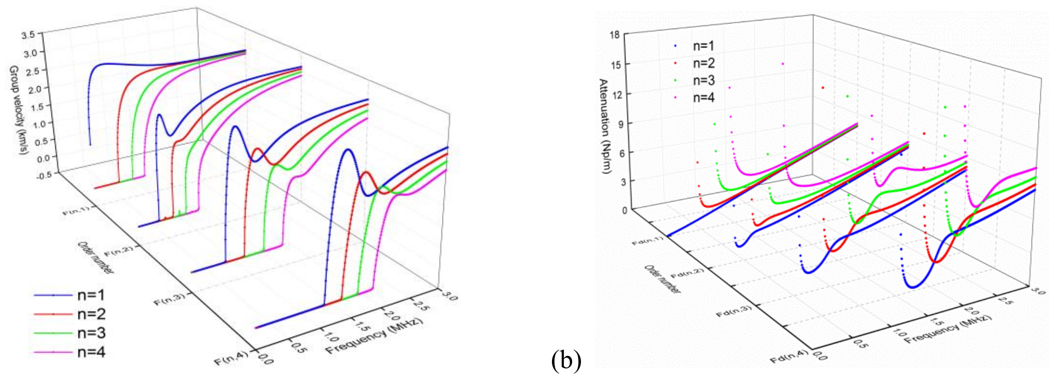


**Figure 3.** Dispersion curves of flexural modes with same $m$

(a) Energy velocity curves; (b) Attenuation coefficient curves

## 4 Initial stress effects on viscoelastic steel wire

In order to clarify the influences of tensile stress on wave characteristics, situations of $0.0, 0.2, 0.4, 0.6, 0.8$ of ultimate tensile strength (UTS, here is $1860MPa$) are analyzed in this section. In terms of wave motion in a pre-stressed waveguide, the virtual work formulation correspondingly is modified as

$$\int_V \left(\delta\boldsymbol{\varepsilon}^T\boldsymbol{\sigma} + \delta\boldsymbol{e}^T\boldsymbol{\sigma}_0\right)dV + \int_V \delta\boldsymbol{u}^T\left(\rho\ddot{\boldsymbol{u}}\right)dV = \boldsymbol{0} \tag{12}$$

in which, $\boldsymbol{e}$ and $\boldsymbol{\sigma}_0$ are non-linear strain field and initial stress field. In the current case, only the axial strain $E_z$ should be considered, which is related to initial axial stress $\sigma_{0z}$, written as

$$E_z = \varepsilon_z + e_z = \left(\frac{\partial u_z}{\partial z}\right) + \left(\frac{1}{2}\left[\left(\frac{\partial u_r}{\partial z}\right)^2 + \left(\frac{\partial u_\theta}{\partial z}\right)^2 + \left(\frac{\partial u_z}{\partial z}\right)^2\right]\right) \tag{13}$$

Finally, it can be readily derived that the effects of $\sigma_{0z}$ is introduced by a geometric stiffness matrix $\boldsymbol{K}_n = \sigma_{0z}\boldsymbol{M}/\rho$ serving as a modification of $\boldsymbol{K}_3$.

Figure 4 illustrates $\Delta C_e$ and $\Delta Att$ of $F_d(n,1)$ modes under four kinds of axial tensile stresses. It is obvious that higher tensile stress is able to accelerate energy velocities and decrease attenuation as well. However, it only happens in relatively high frequency regions which are above cut-off frequencies, noted as the dash lines in the figure. While in low frequency regions, of which modes have extremely high attenuations, even though attenuations are decreased due to tensile stresses, the variations of energy velocities might still be negative, for example the $0 \sim 0.4MHz$ of $F_d(2,1)$ modes. Fortunately, from a practical point of view, only those propagative modes with low attenuation, on which the effects are reasonable and clear, are supposed to be concerned.

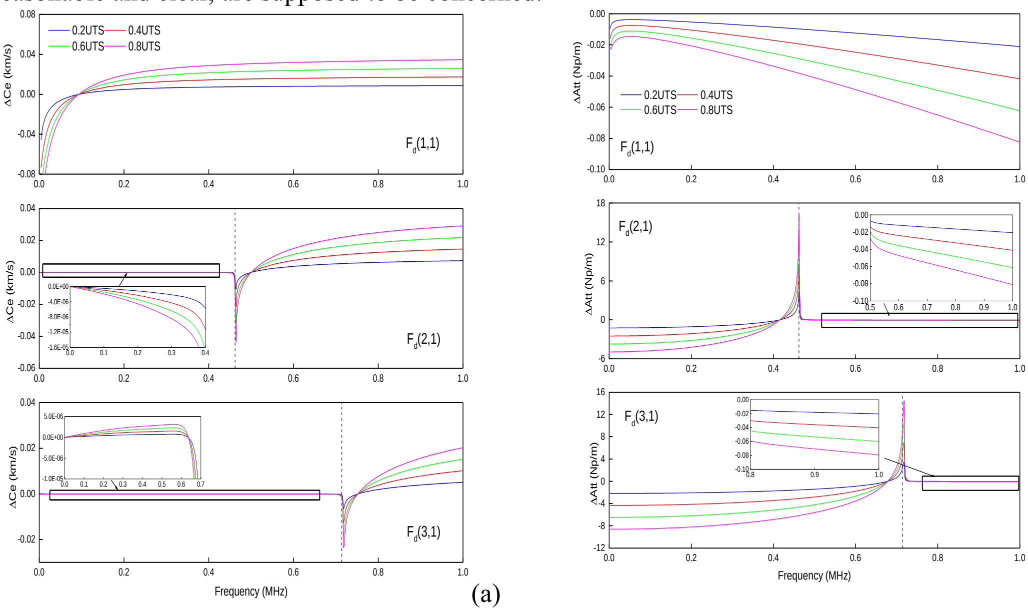


(b)

**Figure 4.** Dispersion curve variations of $\boldsymbol{F_d(n,1)}$ under different initial tensile stress

(a) Energy velocity variations $\Delta C_e\,(km/s)$; (b) Attenuation coefficient variations $\Delta Att\,(Np/m)$

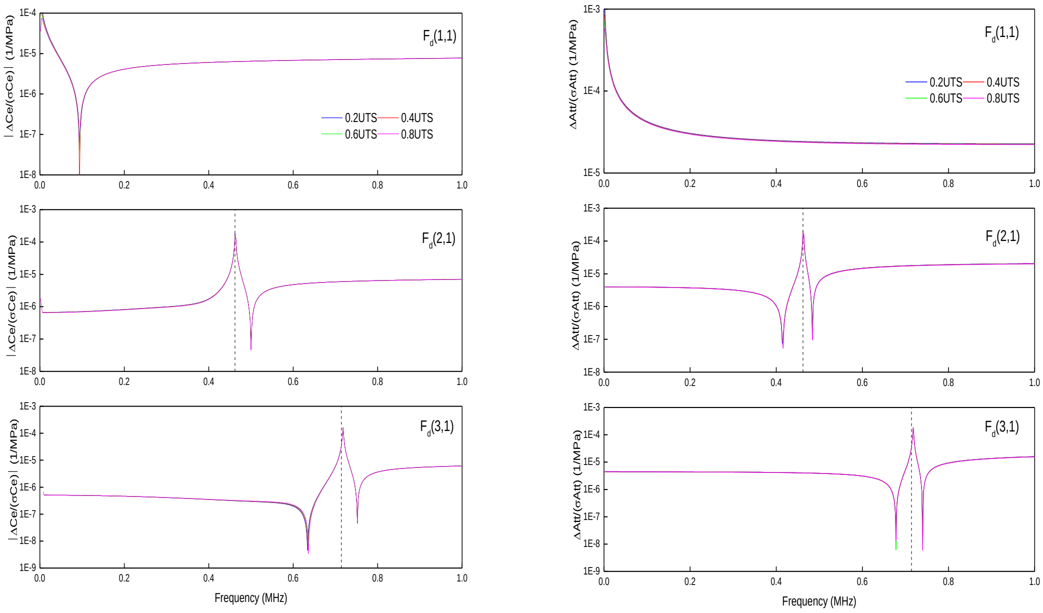


(a) (b)

**Figure 5.** Acoustoelastic constant curves

(a) Absolute value of $S_{C_e}(f)$ ; (b) Absolute value of $S_{Att}(f)$

The effects of tensile stress are monotonous; it increases/decreases a certain trend constantly. It also seems that the effects are linear, since the range of $\Delta C_e$ and $\Delta Att$ curves approximately keep same intervals with each other in each frequency point, though the intervals change along with frequency axis. The so called acoustoelastic constants can be employed to quantify the effects, defined as

$$S_{C_e}(f) = \left( \frac{C_e(f,\sigma) - C_e(f,0)}{C_e(f,0)\sigma} \right) \quad S_{Att}(f) = \left( \frac{Att(f,\sigma) - Att(f,0)}{Att(f,0)\sigma} \right) \tag{14}$$

In Figure 5, all of the four curves in each figure almost coincide together, which indicates the acoustoelastic constants are dependent on frequency only.

## 5 Conclusions

In this paper, the axisymmetric SAFE method has been introduced to analyze the wave characteristics of a high tensile strength steel wire with 5 mm diameter, typically used in bridge cables. The circular cross section is discretized by mono-dimensional elements.

The full frequency spectrums can be solved as general eigenvalue problems for viscoelastic materials. Energy velocities can be readily computed through stiffness and mass matrices. The attenuation curves, which represent the decaying properties of wave modes, could be analyzed. Firstly, they decrease with the increase of frequency up to some minimums which correspond some maximums of energy velocities, and then they increase again and converge into linear tendencies finally. Generally, the curves of modes with same frequency order number $m$ possess similar tendencies.

The effects of axial tensile stress on energy velocities and attenuation have been studied. It turns out that tensile stress could increase and decrease energy velocities and attenuations respectively for most of modes above cut-off frequencies. When it comes to modes with high attenuations, the tensile stress may lead to reverse effects. In general, the effects of tensile stress are linear, quantified as same acoustoelastic constant for different stress levels.

## References

[1] Graff, K.F., *Wave motion in elastic solids*. 1975: Courier Corporation.

[2] Nelson, R., S. Dong, and R. Kalra, *Vibrations and waves in laminated orthotropic circular cylinders.* Journal of Sound and Vibration, 1971. **18**(3): p. 429-444.

[3] Gavrić, L., *Computation of propagative waves in free rail using a finite element technique.* Journal of Sound and Vibration, 1995. **185**(3): p. 531-543.

[4] Hayashi, T., W.-J. Song, and J.L. Rose, *Guided wave dispersion curves for a bar with an arbitrary cross-section, a rod and rail example.* Ultrasonics, 2003. **41**(3): p. 175-183.

[5] Bartoli, I., et al., *Modeling wave propagation in damped waveguides of arbitrary cross-section.* Journal of Sound and Vibration, 2006. **295**(3): p. 685-707.

[6] Marzani, A., et al., *A semi-analytical finite element formulation for modeling stress wave propagation in axisymmetric damped waveguides.* Journal of Sound and Vibration, 2008. **318**(3): p. 488-505.